

Monte Carlo simulations of the OSIRIS and IRIS
neutron spectrometers using the virtual neutron
instrumentation tool, VITESS

M.T.F.Telling

ISIS Facility,
Rutherford Appleton Laboratory,
Chilton,
Didcot,
Oxfordshire,
OX11 0QX

August 2004

ABSTRACT

The development of the OSIRIS neutron instrument on the ISIS pulsed source is a three-phase process; namely the sequential realisation of high-resolution diffraction, low-energy spectroscopy and full polarisation analysis capabilities on the spectrometer. With the recent completion of the second phase, the instrument now affords the option of high-resolution quasi-elastic and low-energy inelastic neutron spectroscopy.

The performance of the OSIRIS spectrometer, and a full description of the instrument, is presented in technical report RAL-TR-2004-005, the spectroscopic characteristics of the instrument being discussed in terms of energy resolution, neutron count rate and signal-to-background ratio as well as being compared to the spectroscopic capabilities of the near-backscattering spectrometer, IRIS.

However, it is becoming common practise to benchmark neutron instruments using Monte Carlo methods. In this report, the observed, and previously reported, operation of the complete OSIRIS instrument is compared and contrasted to the simulated response of the complete spectrometer using the virtual instrumentation tool for neutron scattering at pulsed and continuous sources, VITESS; comparisons being made in terms of energy resolution. The results for OSIRIS are also likened to the simulated, and operational, performance of the IRIS spectrometer to ascertain comparative neutron count rates.

CONTENTS

I. Introduction	4
II. Simulation Procedure	5
III. Results	11
IV. Discussion	14
V. Reference	15
Appendix I. VITESS Instrument Descriptions	16
Appendix II. Detector Efficiency	23
Appendix III. Reflectivity Calculations	24
Appendix IV. Open Genie Procedure	26
Appendix V. Vanadium Scattering Coefficient	28
Appendix VI. OSIRIS PG Analyser Description	29
Appendix VII. C.A.D Drawings	30

I. INTRODUCTION

The development of the OSIRIS neutron instrument on the ISIS pulsed source is a three-phase process; namely the sequential realisation of high-resolution diffraction, low-energy spectroscopy and full polarisation analysis capabilities on the spectrometer. With the recent completion of the second phase, the instrument now affords the option of high-resolution quasi-elastic and low-energy inelastic neutron spectroscopy.

The performance of the complete OSIRIS spectrometer, and a full description of the instrument, has been presented in technical report RAL-TR-2004-005 [1] and [2]; the spectroscopic characteristics of the instrument being discussed in terms of energy resolution, neutron count rate and signal-to-background ratio as well as being compared to the spectroscopic capabilities of the near-backscattering spectrometer, IRIS.

However, it is becoming common practice to benchmark the response of a neutron instrument using Monte Carlo simulation techniques. In this report, the observed, and previously reported, operation of the complete OSIRIS instrument is compared and contrasted to the predicted response of the complete spectrometer generated using the neutron instrument simulation package, VITESS [3]; comparisons being made in terms of energy resolution. The parameters used to fully describe the OSIRIS instrument in VITESS are tabulated in Appendix 1. In addition, the results for OSIRIS are also likened to the simulated performance of the IRIS spectrometer to ascertain comparative neutron count rates.

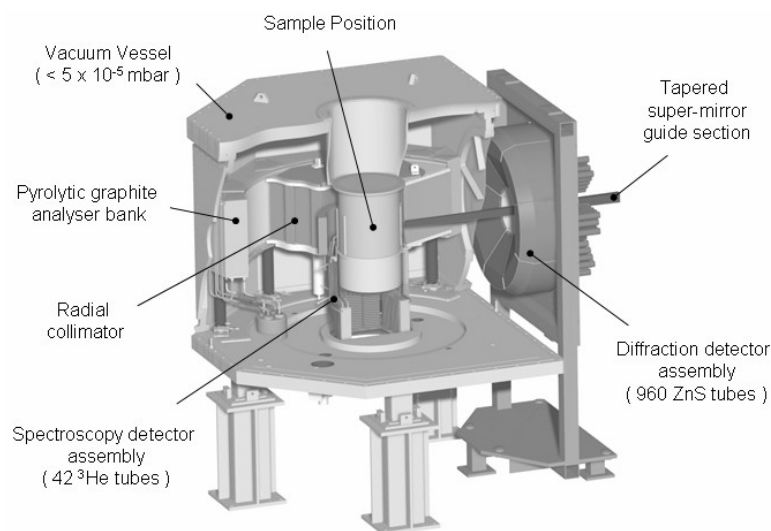


Figure 1. *The OSIRIS spectrometer at the ISIS Facility, Rutherford Appleton Laboratory, UK*

Should the results presented here been seen to demonstrate a satisfactory agreement between the virtual and experimental instrument performances then the simulations will be used as a blue print for the development of TS2 backscattering instruments.

II. SIMULATION PROCEDURE

Simulations were performed using the neutron instrumentation simulation package, VITESS (version 2.5) [3]. This package can be downloaded, and installed, from the VITESS homepage (<http://www.hmi.de/projects/ess/vitess/>). The simulations were run on a desktop PC (3 GHz) running Windows XP. A Unix version of the package is also available. Typically, a simulation would take between 4 – 8 hours. A comprehensive description of the VITESS package can be found at <http://www.hmi.de/projects/ess/vitess/DOC/vitess.html>.

The parameters required by VITESS to fully describe the OISRIS and IRIS instruments were determined, wherever possible, from Computer Aided Design (CAD) drawings of the two spectrometers; these parameters being tabulated in full in Appendix I. The CAD drawings from which these values were evaluated are shown in Appendix VI. In the few cases where no CAD information was available, measurements were made by hand on the instruments.

It has also been possible to compare VITESS energy resolution results for the IRIS spectrometer to energy resolution simulations generated using MC code developed at ISIS by Dr Stuart Campbell [4]. Written in-house, the code, named Animal, was written in FORTRAN 90, with a IDL graphical user interface, and employed to optimise the cross sectional profile of the graphite analyser bank currently used on the IRIS instrument.

In brief, a description of a complete neutron instrument is built up using individual modules – from neutron guide sections to detector assemblies. VITESS treats each module individually, simulating the passage of ‘N’ different neutron trajectories through a component before passing, or piping, the number transmitted through that element to the subsequent module. For simplicity neutron trajectories will be simply referred to as neutrons from here on in. The VITESS components required to describe the complete OSIRIS neutron guide are shown in Figure 2. The majority of the modules used are self explanatory and require simple input parameters, these values being obtained from CAD drawings. However, a few elements require additional information to be calculated, such as the graphite analyser. Such supplementary information will now be discussed.

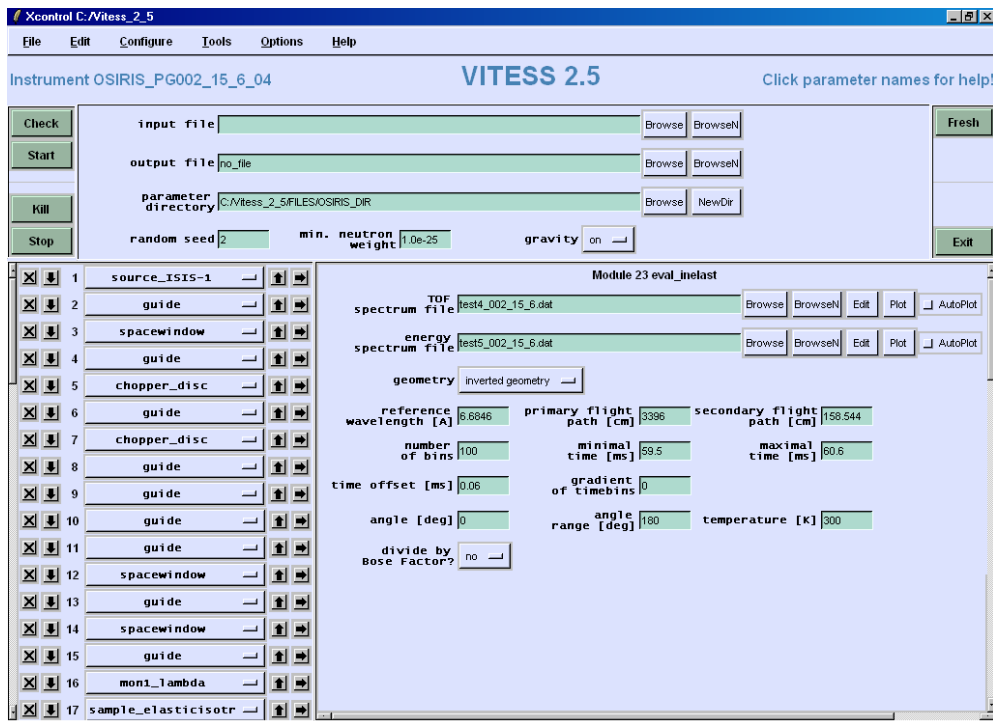


Figure 2. The OSIRIS 'primary' spectrometer as delineated in VITESS

1. The Pyrolytic Graphite Analyser Bank

- The VITESS code allows the user the option of using either a spherical analyser profile, generated internally by the program, or an analyser profile description file created by the user. Since both the OSIRIS and IRIS analysers favour the geometry of an ellipse [4] a user generated description file was created from CAD drawings depicting the position and orientation of each individual analyser crystal (see Appendix VI)
- The OSIRIS and IRIS instruments operate with radial collimators between their sample position and analyser bank. A collimator module was not included in the VITESS description of the instruments. However, to mimic the effect of collimation, the width of the analyser viewed by the sample was limited to a segment 3 crystal pieces wide in the analyser profile description file for both instruments.
- The actual OSIRIS analyser is 40 crystal pieces high and, as such, the instruments radial collimator is optimised such that all 40 pieces are viewed by the sample. However, while the IRIS analyser is physically 18 graphite crystals high, only 13 are viewed by the

sample due to the limiting geometry of the IRIS radial collimator – the scattered beam missing the bottom 5 rows. As a result, for IRIS, the analyser description file generated only considered the 13 crystal elements seen by the sample.

- To enable comparative neutron count rates to be ascertained between the two spectrometers, it was necessary to scatter virtual neutrons on both instruments from the sample position into areas of the same magnitude. This area was defined by the larger of the two analysers.
- The reflectivity of pyrolytic graphite as a function of neutron wavelength is not calculated by the VITESS code; although the number of neutrons Bragg reflected by an analyser can be normalised to a proportionate value for the case when, for example, two different analyser materials are used. However, the OSIRIS and IRIS graphite crystals used on the instruments are 0.2cm and 0.1cm thick respectively. It was therefore necessary to determine whether reflectivity varied significantly as a function of crystal thickness i.e. would crystal depth notably affect neutron count rate. Reflectivity values for the two crystal types are tabulated below. Details of the reflectivity calculation are given in Appendix III.

	PG002 ($\lambda \sim 6.66 \text{ \AA}$)	PG004 ($\lambda \sim 3.33 \text{ \AA}$)
Reflectivity, R (0.1 cm crystal at RT)	0.986	0.925
Reflectivity, R (0.2 cm crystal at RT)	0.981	0.908

Table 1. *Reflectivity values for 0.1cm and 0.2cm thick pyrolytic graphite analyser crystals and at different wavelengths*

Calculation shows that there was very little difference in reflectivity between a 0.1 and 0.2cm thick PG crystal. Consequently, no correction was made for reflectivity in the results presented.

- Average Bragg angle, secondary flight path and analysed neutron wavelength values, used to evaluate energy transfer and total time of flight ranges for the detected neutron trajectories, are tabulated below.

	OSIRIS analyser	IRIS analyser
Mean secondary flight path (mm)	1585.44	1450.88
Mean Bragg angle (deg)	4.6526	4.96
Mean analysed wavelength PG002 (A)	6.6846	6.6827
PG004 (A)	3.3423	3.3413
Size of analyser used in the simulation	40 graphite crystals high by 3 graphite crystals wide	13 graphite crystals high by 3 graphite crystals wide

Table 2. Average Bragg angle, secondary flight path and analysed wavelength values for the OSIRIS and IRIS analyser profiles

2. OSIRIS and IRIS Detector Assemblies

- Bragg reflected neutrons were detected by modelling single ^3He (OSIRIS), or ZnS (IRIS), detectors.
- Selecting the “Standard Frame Generation” option in the ‘analyser’ module automatically focussed the energy analysed beam to a point along the Bragg scattering direction. The detectors were therefore located at a user defined distance ‘X’ meters along the scattered beam direction.
- The active area of the detector was automatically oriented perpendicular to, and centred about, the scattered beam direction. In practice, the OSIRIS and IRIS detectors are inclined such that this is approximately the case on the instruments.

- The position of the OSIRIS detector assembly and dimensions of each ^3He detector tube were ascertained from CAD drawings. The tubes modelled are ½-inch diameter, 10 atmosphere, cylinders with an active length of 3.912cm
- The wavelength dependant efficiencies of a ^3He and a ZnS detector are illustrated in Appendix II
- No detailed CAD drawing exists of the actual IRIS detector assembly. The dimensions of a single ZnS detector had to be obtained from Dr Nigel Rhodes - the detector parameters required by VITESS determined by measuring an old prototype IRIS detector. The IRIS detector is made up of six 12mm (high) x 12mm (wide) by 1mm (thick) pieces of ZnS material. The slabs are oriented at approximately 42° with a 5mm pitch between each piece. The total active area is 5.2cm

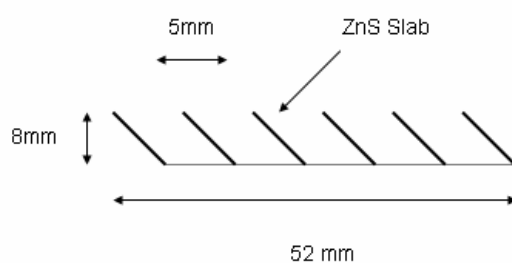


Figure 3. Schematic diagram of a single IRIS ZnS detector

- Position sensitive detector modules were incorporated into the instrument descriptions to ensure that the energy analysed beam was focussed at the virtual detector position. This was found to be the case, the maximum intensity of the detected beam falling at the centre of the detector (see Figure 4). In fact, simulation suggests that the detector positions on both instruments could be optimised to improve neutron count rate further.

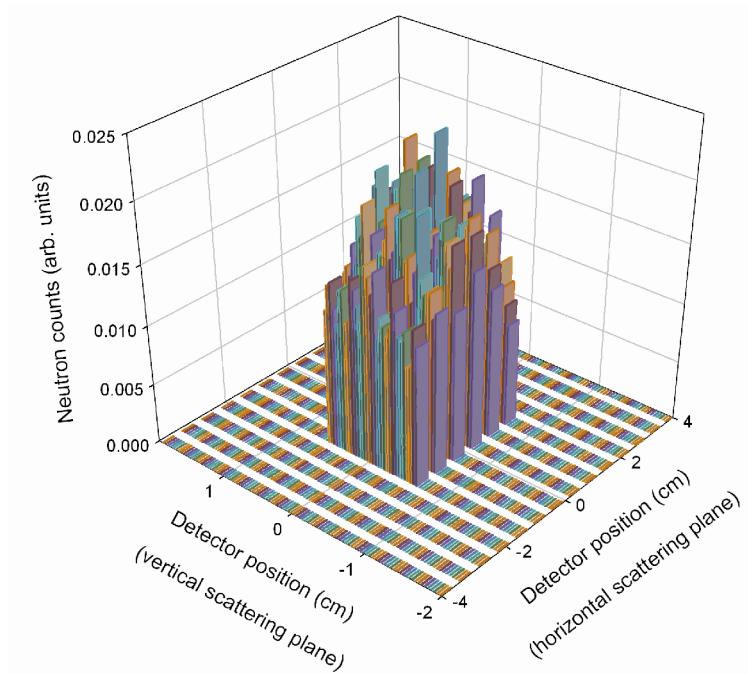


Figure 4. *Distribution of detected neutrons across the OSIRIS detector area*

3. Cylindrical Sample

- OSIRIS and IRIS energy resolution measurements were collected using the same thin-walled annular vanadium standard – this standard being comprised of three concentric 0.04mm thick cylinders of diameter 1cm, 1.6cm and 2cm. Total thickness of vanadium in the beam is 0.024cm
- At present, VITESS is not able to simulate scattering from a hollow cylinder. Instead a solid cylinder is assumed whose diameter is defined by the user; in this case 2cm.
- Such a dense sample demonstrates strong wavelength dependant neutron absorption. To alleviate this, the absorption cross section of the sample was assumed to be zero. Since, in the first instance, comparison of the simulated neutron count rate between the two instruments was relative, rather than absolute, the absorption value used was not critical providing it was constant for all simulations. In addition, zero absorption not only improved statistics but also reduced the simulation running time.
- For a solid, 2cm diameter vanadium sample, the scattering coefficient was calculated to be 0.369 cm^{-1} (see Appendix V)

IV. Results

Results are shown in Figures 5 to 7 and tabulated in table 4. Simulated OSIRIS and IRIS neutron count rates for both the PG002 and PG004 instrument configurations are shown below in Figure 5. All simulation presented here were performed using 50 billion neutron trajectories and setting ‘repetition’ equal to 1 in the analyser, sample and detector modules. Experimentally determined instrument neutron count rates are shown for comparison in Figure 6.

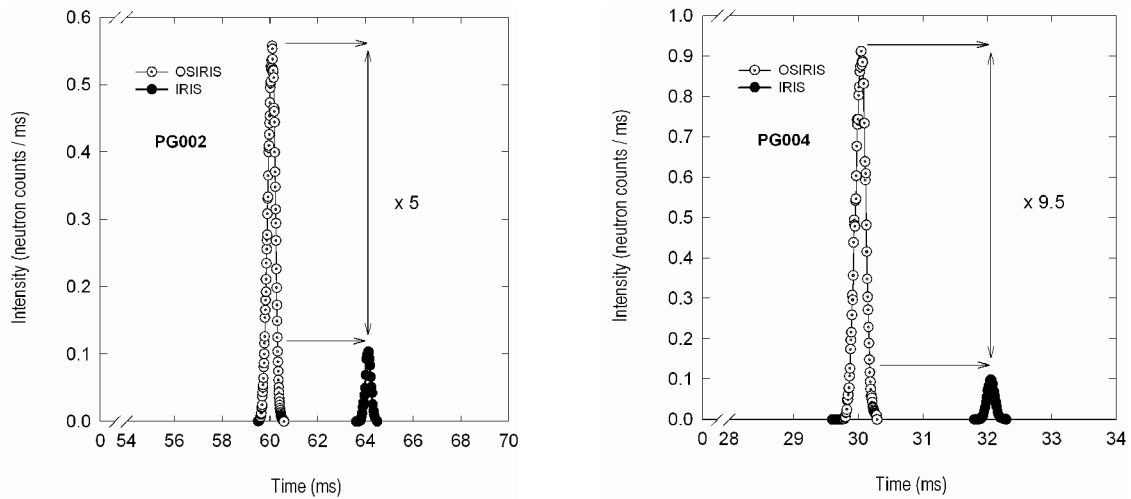


Figure 5. Simulated OSIRIS and IRIS neutron count rates per millisecond for PG002 and PG004

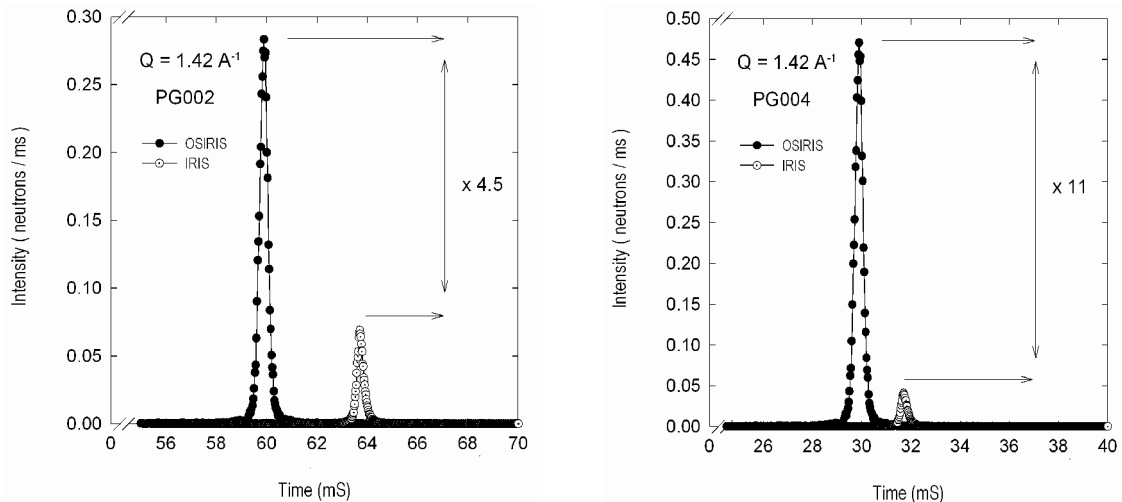


Figure 6 Experimental OSIRIS and IRIS neutron count rates per millisecond for PG002 and PG004[2]

For PG002, comparison of the number of virtual neutrons detected in the elastic channel ($\Delta E=0$) per millisecond from each spectrometer highlights a 5-fold increase in neutron count rate on OSIRIS compared to IRIS. Such an increase is predominantly the multiplicative consequence of i) the approximate 2-fold increase in the number energy analysed neutrons transported from moderator to sample position on OSIRIS [2] and ii) the approximate 3-fold increase in vertical elongation of the OSIRIS (40cm high) analyser compared to that installed on IRIS (13cm high). For PG004, OSIRIS simulations show a 9.5-fold increase in count rate compared to IRIS. These results are in good agreement with the gains observed in Figure 6, experimentally determined values suggesting 4.5 and 11-fold increases in neutron count rate on OSIRIS compared to IRIS for PG002 and PG004 respectively.

OSIRIS and IRIS experimental energy resolution data and corresponding Monte Carlo simulation results for PG002 are compared in Figure 7. The IRIS PG002 results are also likened to spectra generated using the in-house MC package, Animal (see section III and [4])

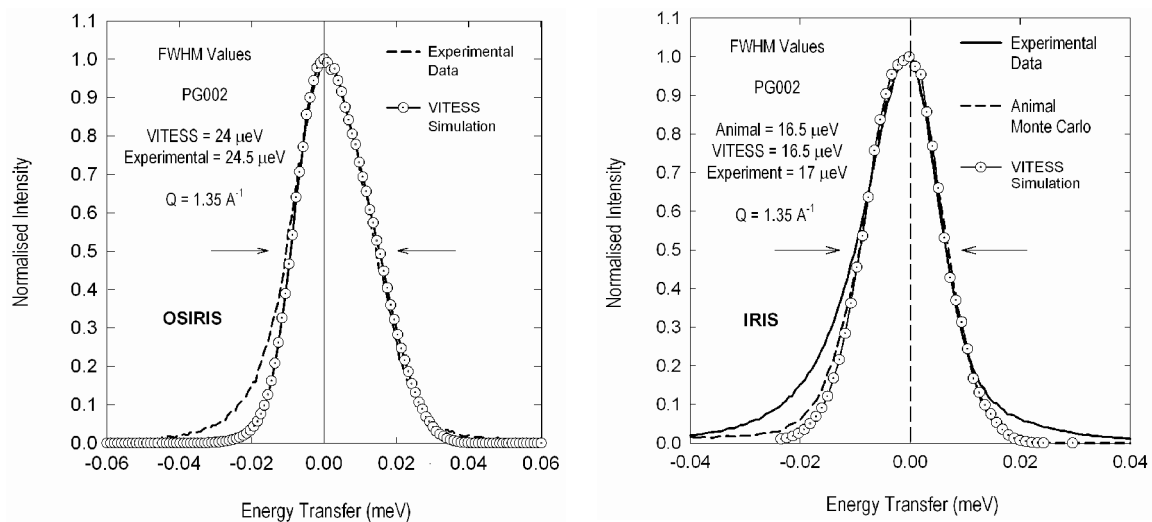


Figure 7. Comparison of simulated and measured OSIRIS (left) and IRIS (right) instrument energy resolution function for the PG002 analysing reflection

The discrepancy at the base of the elastic line is a consequence of Thermal Diffuse Scattering (TDS) [5]. This background component is an intrinsic temperature dependant property of pyrolytic graphite but can not as yet be modelled by the VITESS package [3]. Nevertheless, the form and breadth at full width half maximum (fwhm) of both elastic line data sets are in good agreement. For PG002, comparison of energy resolution simulations for OSIRIS and IRIS does highlight an approximate $7\mu\text{eV}$ difference in the breadth of the elastic

line at full width half maximum, i.e. $24\mu\text{eV}$ (OSIRIS, simulated) compared to $16.5\mu\text{eV}$ (IRIS,simulated). Similarly, for PG004, a variance in fwhm of $42\mu\text{eV}$, from $54\mu\text{eV}$ (IRIS, simulated) to $96\mu\text{eV}$ (OSIRIS, simulated), is seen. This unavoidable reduction in energy resolution on OSIRIS is observed in the experimental data and is a consequence of the marked increase in vertical extension of the OSIRIS analyser (40 cm high) out of the horizontal scattering plane when compared to the IRIS analyser (13 cm high).

	OSIRIS Monte Carlo VITESS	OSIRIS Experimental (Analyser at 8K)	IRIS Monte Carlo VITESS	IRIS Experimental (Analyser at 12K)
FWHM of Elastic Line				
PG002 (μeV)	24	24.5	16.5	17
PG004 (μeV)	96	99	54	55
OSIRIS neutron count rate (relative to IRIS value)				
PG002	x 5	x 4.5	x 1	x 1
PG004	x 9.5	x 11	x 1	x 1

Table 4. A comparison of the simulated and operational performance of the OSIRIS and IRIS

IV. Discussion

It is becoming common practice to benchmark the performance of a neutron instrument using Monte Carlo simulation techniques. In this report, the observed, and previously reported [1], operation of the complete OSIRIS instrument has been compared and contrasted to the predicted response of the complete spectrometer generated using the neutron instrument simulation package, VITESS [3]. The OSIRIS results are also likened to the simulated performance of the near-backscattering spectrometer, IRIS, to ascertain comparative neutron count rates.

For both spectrometers, experimental PG002 and PG004 energy resolution measurements are in good agreement with predictions made for the performance of the complete instruments using VITESS. In addition, IRIS PG002 energy resolution simulations generated using VITESS are also comparable to virtual results generated using the in-house Monte Carlo package, Animal.

However, comparison of simulated neutron count rates between the two spectrometers shows a 5-fold and 9-fold increase in number of detected neutrons per millisecond on OSIRIS for PG002 and PG004 respectively compared to IRIS. These results are in good agreement with the gains observed on the actual instruments, experimentally determined values suggesting 4.5 and 11-fold increases in neutron count rate on OSIRIS compared to IRIS for PG002 and PG004 respectively.

The results presented in this report demonstrate that a satisfactory agreement has been reached between the virtual performance and experimental operation of the two neutron instruments. As a result, these OSIRIS and IRIS simulations will be used as a blue print for the development of TS2 backscattering instruments such as the proposed HERBI spectrometer.

V. References

1. M.T.F.Telling *et al*, *Performance of the cooled pyrolytic graphite analyser bank on the OSIRIS spectrometer at ISIS*, RAL-TR-2004-05
2. M.T.F.Telling and K.H.Andersen, *Spectroscopic characteristics of the OSIRIS spectrometer on the ISIS pulsed source*, *Physical Chemistry Chemical Physics*, Proceedings of QENS 2004 conference
3. D. D. Wechsler *et al*, *Monte Carlo simulations for instrumentation at pulsed and continuous sources*, Proceedings of ECNS-II, *Physica B* 276-278 (2000) 71-72.
4. S.I.Campbell *et al*, *The new IRIS pyrolytic graphite analyser*, *Physica B*, 2000, **276-278**, 206
5. C.J.Carlile *et al*, *Less background, better contrast by cooling analyser crystals*, *Nucl Instrum Meth A* **338** 78 (1994)

Appendix I. VITESS Instrument Descriptions

All instrument parameters have been determined, where possible, from CAD drawings of the spectrometers. Where no CAD information is available measurements have been made by hand. The CAD drawings used are shown in Appendix VI

The OSIRIS spectrometer

I. Moderator Parameters

Moderator file used	Dist of moderator from first guide piece	User wavelength time distribution file used	Moderator width and height (cm) and temperature (K)	Total flux at moderator (n/cm/s)	Min and max time (ms) and divergence (deg)	Direction defined, propagation window width and height (cm)
<i>ISISTS1 Hyrdogen.mod</i>	<i>169.8</i>	<i>Vit.iris</i>	<i>10, 10, 25</i>	<i>1.1×10^{-13}</i>	<i>0, 0.48, 0.5 0.5</i>	<i>By window, 4.3, 6.5</i>

II. The OSIRIS 'primary' Spectrometer

	Length of each guide piece (cm)	Entry Width and Height (cm)	Exit Width and Height (cm)	Horizontal and Vertical shape	Radius of curvature (cm)	No. of pieces	'm' file used
Guide	<i>200</i>	<i>4.3 / 6.5</i>	<i>4.3 / 6.5</i>	<i>constant / constant</i>	<i>0</i>	<i>1</i>	<i>mirr2</i>
Space window	<i>See</i>	<i>space</i>	<i>window</i>	<i>1</i>	<i>description</i>	<i>below</i>	<i>-</i>

Guide	247.8	4.3 / 6.5	4.3 / 6.5	<i>constant / constant</i>	0	1	<i>mirr2</i>
Chopper	<i>See</i>	6m	chopper	description	below	-	-
Guide	184	4.3 / 6.5	4.3 / 6.5	<i>curved / constant</i>	2050	2	<i>mirr2</i>
Chopper	<i>See</i>	10m	chopper	description	below	-	-
Guide	353.735	4.3 / 6.5	4.3 / 6.5	<i>curved / constant</i>	2050	2	<i>mirr2</i>
Guide	348.95	4.3 / 6.5	4.3 / 6.5	<i>curved / constant</i>	2050	2	<i>mirr2</i>
Guide	340.95	4.3 / 6.5	4.3 / 6.5	<i>curved / constant</i>	2050	2	<i>mirr2</i>
Guide	21.25	4.3 / 6.5	4.3 / 6.5	<i>curved / constant</i>	2050	2	<i>mirr2</i>
Space window	<i>See</i>	space	window	2	description	below	-
Guide	60	4.3 / 6.5	4.3 / 6.5	<i>constant / constant</i>	0	1	<i>mirr2</i>
Space window	<i>See</i>	space	window	3	description	below	-
Guide	150.63	4.3 / 6.5	2.2 / 4.4	<i>linear / linear</i>	0	1	<i>mirr3+</i>

III. 6 and 10m Chopper Parameters

	Disk chopper file used	Rounds /min	Offset (002, 004, deg)	Dist to previous guide piece (cm)	No. of windows	Radius (cm)	Vert / Horizontal position of axle (cm)	Window height (cm) / width (deg)
6m	<i>Chop3_6.chp</i>	3000	-281, -185	4.04	1	30.8	0 / 28	9.1 / 66
10m	<i>Chop10.chp</i>	-3000	213, 60	1.05	1	30.8	0 / 28	9.1 / 98

IV. Space Window Parameters

	Distance to window from last guide section (cm)	Shape	Radius (cm)	Material	Inner thickness of material (cm)	Outer thickness of material (cm)
1	6.6	<i>Circular</i>	30	<i>Ideal absorber</i>	0	0
2	8.76	<i>Circular</i>	30	<i>Ideal absorber</i>	0	0
3	17.8	<i>Circular</i>	25	<i>Ideal absorber</i>	0	0

V. OSIRIS Sample Parameters

Module used	Angle hor / vert (deg)	Δ angle hor / vert (deg)	Scat coeff. (cm^{-1})	Abs coeff. ($1/\text{cm}/\text{A}$)	*Sampl e position x, y, z (cm)	Sampl egeom.	Sample diameter, height, width (cm)	Output frame x',y',z' (cm)
<i>Sample_elasticisotr</i>	0, 0	2, 27	0.368	1e-10	25, 0, 0	Cyl	2.2, 4.4, 2.2	25, 0, 0

* Relative to end of neutron guide

VI. OSIRIS Graphite Analyser Parameters

Module used	Mosaicity hor / vert (deg), mosaic range factor	d spread and distribution	Main position x, y, z (cm)	Surface offset hor/vert (deg)	Bragg offset hor/vert (deg)	Crystal thickness, width, height (cm)	d-spacing (A), d range factor
<i>ma_focus_dat</i>	0.8, 0.8, 1000	0.0025, gaussian	90.68, 0, 0	0, 0	0, 4.6526*	0.2, 1, 1	3.354(002), 1.677(004), 5

Output frame generated by internal code using option “Standard Frame Generation”

* A ‘Bragg Offset Angle (vert)’ is used here in conjunction with “Standard Frame Generation” to allow actual detector dimensions to be simulated

Graphite crystal position and orientation file generated using CAD drawing of analyser profile

VII. OSIRIS ^3He Detector Parameters

Module used	Geometry	Effective height, width and thickness (cm)	Efficiency (002,004), theta (deg) and phi (deg)	Distance (cm)	No. of columns, rows
<i>Detector</i>	<i>flat</i>	3.912, 1.27, 1.27	0.973 (002), 0.89 (004), 0, 0	67	1, 1

The IRIS spectrometer

III. Moderator Parameters

Moderator file used	Dist of moderator from first guide piece	User wavelength time distribution file used	Moderator width and height (cm) and temperature (K)	Total flux at moderator (n/cm/s)	Min and max time (ms) and divergence (deg)	Direction defined, propagation window width and height (cm)
<i>ISISTS1 Hydrogen.mod</i>	<i>158.3</i>	<i>Vit.iris</i>	<i>10, 10, 25</i>	<i>1.1 x10⁻¹³</i>	<i>0, 0.48, 0.5 0.5</i>	<i>By window, 4.5, 6.7</i>

IV. The IRIS 'primary' Spectrometer

	Length of each guide piece (cm)	Entry Width and Height (cm)	Exit Width and Height (cm)	Horizontal and Vertical shape	Radius of curvature (cm)	No. of pieces	'm' file used
Guide	<i>449.8</i>	<i>4.5 / 6.7</i>	<i>4.3 / 6.5</i>	<i>linear / linear</i>	<i>0</i>	<i>1</i>	<i>mirr1b</i>
Chopper	<i>See</i>	<i>6m</i>	<i>chopper</i>	<i>description</i>	<i>below</i>	<i>-</i>	<i>-</i>
Guide	<i>84.825</i>	<i>4.3 / 6.5</i>	<i>4.3 / 6.5</i>	<i>curved / constant</i>	<i>2350</i>	<i>4</i>	<i>mirr1b</i>
Chopper	<i>See</i>	<i>10m</i>	<i>chopper</i>	<i>description</i>	<i>below</i>	<i>-</i>	<i>-</i>

Guide	98.33	4.3 / 6.5	4.3 / 6.5	<i>curved / constant</i>	2350	24	<i>mirr1b</i>
Guide	250	4.3 / 6.5	2.2 / 3.2	<i>linear / linear</i>	0	1	<i>mirr2linear</i>

VIII. 6 and 10m Chopper Parameters

	Disk chopper file used	Rounds /min	Offset (deg)	Dist to previous guide piece cm	No. of windows	Radius (cm)	Vert / Horizontal position of axle (cm)	Window height (cm) / width (deg)
6m	<i>Chop3_6.chp</i>	3000	-280	19.8	1	30.8	0 / 28	9.1 / 60
10m	<i>Chop10.chp</i>	-3000	210	19.8	1	30.8	0 / 28	9.1 / 100

IX. IRIS Sample Parameters

Module used	Angle hor / vert (deg)	Δ angle hor / vert (deg)	Scat coeff. (cm^{-1})	Abs coeff. ($1/\text{cm}/\text{A}$)	*Sample position x, y, z (cm)	Sample geom.	Sample diameter, height, width (cm)	Output frame x',y',z' (cm)
<i>Sample_elasticisotr</i>	0, 0	2, 27	0.368	1e-10	44, 0, 0	<i>Cyl</i>	2.2, 3.3, 2.2	44, 0, 0

* Relative to end of neutron guide

X. IRIS Graphite Analyser Parameters

Module used	Mosaicity hor / vert (deg), mosaic range factor	d spread and distribution	Main position x, y, z (cm)	Surface offset hor/ vert hor (deg)	Bragg offset hor/ vert (deg)	Crystal thickness, width, height (cm)	d-spacing (Å), d range factor
<i>ma_focus_dat</i>	<i>0.8, 0.8, 1000</i>	<i>0.0025, gaussian</i>	<i>85, 0, 0</i>	<i>0, 0</i>	<i>0, 4.96*</i>	<i>0.1, 1, 1</i>	<i>3.354(002), 1.677(004), 5</i>

Output frame generated by internal code using option “Standard Frame Generation”

* A ‘Bragg Offset Angle (vert)’ is used here in conjunction with “Standard Frame Generation” to allow actual detector dimensions to be simulated

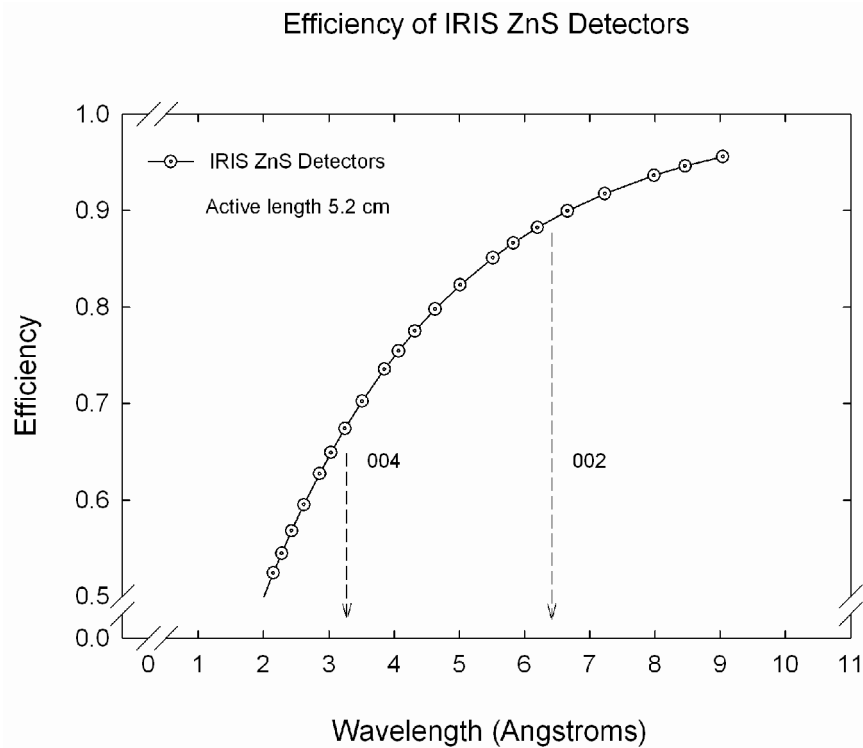
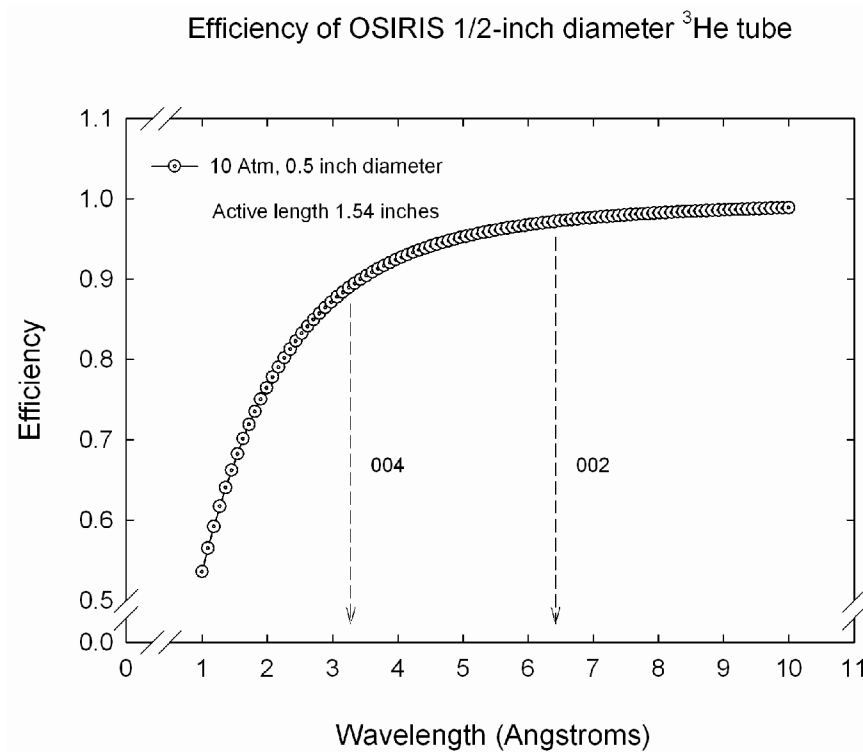
Graphite crystal position and orientation file generated using CAD drawing of analyser profile

XI. IRIS ZnS Detector Parameters

Module used	Geometry	Effective height, width and thickness (cm)	Efficiency (002, 004), theta and phi	Distance (cm)	No. of columns, rows
<i>Detector</i>	<i>flat</i>	<i>5.2, 1.2, 0.1</i>	<i>0.9(002), 0.68(004), 0, 0</i>	<i>60</i>	<i>1, 1</i>

Appendix II. Detector Efficiency

The wavelengths Bragg reflected by the 002 and 004 crystal planes are shown



Appendix III. Reflectivity Calculations

All calculations assume angles are in RADIANS.

For a symmetric Bragg reflection i.e. angle of incidence = angle of reflection the reflectivity of a crystal is given by:

$$R = \frac{b}{([a(a+2b)]^{1/2} \coth[a(a+2b)]^{1/2} + (a+b))}$$

where $a = \mu t$ and $b = \sigma t$

μ = the attenuation coefficient (cm^{-1})

σ = the Bragg reflection coefficient (cm^{-1})

t = thickness of the crystal along the incident beam direction

1. *The attenuation coefficient*

$$\mu = \frac{1}{V_o} \sum (\sigma_c f(x) + \sigma_i + \sigma_a)$$

where $f(x) = 1 - (1 - \exp(-x))/x$ and $x = \left(\frac{4\pi\mu_o}{\lambda} \right)^2$

The sum is over all atoms in the unit cell

σ_c = bound coherent scattering length for an atom in the unit cell which for PG = 5.55 barn

σ_i = bound incoherent scattering cross section which for PG = 0.001 barn

σ_a = absorption cross section which for PG = 0.0035 barn at 1.8 angstroms

V_o = volume of the unit cell which for PG = $35.2 \times 10^{-24} \text{ cm}^3$

μ_o = root mean square displacement of an atom which for PG = 0.33 angstroms (for displacement parallel to the c-axis)

2. *The Bragg reflection coefficient*

$$\sigma = QW(\theta' - \theta)$$

where $W(\theta' - \theta) = 1 / \text{mosaic spread of crystal} (1 / 0.8^\circ)$

$$Q = \lambda^3 |F_{hkl}|^2 / V_o^2 \sin(2\theta)$$

and

$$F_{hkl} = \sum b_c \exp(-W_{hkl}) \exp[2\pi i(hx + ky + lz)]$$

where b_c = bound coherent scattering length which for PG = 6.646 fm

For graphite:

$$F_{hkl,002} = 2.58 \times 10^{-12} \text{ cm}$$

$$F_{hkl,004} = 2.57 \times 10^{-12} \text{ cm}$$

Appendix IV. Open Genie Procedure

Procedure REFLECTIVITY calculates symmetric Bragg reflection reflectivity values for analyser crystals of differing thickness using the theory given in Appendix III. Values are returned for the case of a) neutron absorption and b) no neutron absorption. Silicon and Pyrolytic Graphite crystal values are hard wired into the code.

Appendix V. Vanadium Scattering Coefficient

Fundamental properties of vanadium were obtained from various chemistry web pages e.g.

<http://www.webelements.com/webelements/elements/text/V/>

$$\text{Density of vanadium} = 6110 \text{ kg/m}^3$$

$$\text{Scattering cross section of vanadium} = 5.1 \text{ barns (x } 10^{-24} \text{ cm}^2)$$

$$\text{Molar volume of vanadium} = 8.55 \text{ cm}^3/\text{mol}$$

$$\text{Avogadro's constant} = 6.022 \times 10^{23} \text{ atoms/mol}$$

$$\text{Therefore, number density of one mole of vanadium} = 6.022 \times 10^{23} / 8.55 \text{ cm}^3/\text{mol}$$

$$= 7.23 \times 10^{22} \text{ atoms / cm}^3$$

$$\text{Consequently, the vanadium scattering coefficient} = 7.23 \times 10^{22} \text{ atoms / cm}^3 \times 5.1 \times 10^{-24} \text{ cm}^2$$

$$\text{Vanadium scattering coefficient} = 0.369 \text{ cm}^{-1}$$

Appendix VI. OSIRIS PG Analyser Description

OSIRIS graphite crystal positions/orientations for an analyser element: 1 column x 40 rows

1 40							
-0.7956	0.0000	-20.0000	0.0000	0.0000	0.0000	0.0000	-8.9280
-0.6386	0.0000	-19.0000	0.0000	0.0000	0.0000	0.0000	-8.9280
-0.4814	0.0000	-18.0000	0.0000	0.0000	0.0000	0.0000	-8.9280
-0.3511	0.0000	-17.0000	0.0000	0.0000	0.0000	0.0000	-7.3330
-0.2315	0.0000	-16.0000	0.0000	0.0000	0.0000	0.0000	-6.7910
-0.1124	0.0000	-15.0000	0.0000	0.0000	0.0000	0.0000	-6.7910
-0.0230	0.0000	-14.0000	0.0000	0.0000	0.0000	0.0000	-5.0050
0.0589	0.0000	-13.0000	0.0000	0.0000	0.0000	0.0000	-4.6600
0.1404	0.0000	-12.0000	0.0000	0.0000	0.0000	0.0000	-4.6600
0.1896	0.0000	-11.0000	0.0000	0.0000	0.0000	0.0000	-2.7030
0.2339	0.0000	-10.0000	0.0000	0.0000	0.0000	0.0000	-2.5300
0.2781	0.0000	-9.0000	0.0000	0.0000	0.0000	0.0000	-2.5300
0.2875	0.0000	-8.0000	0.0000	0.0000	0.0000	0.0000	-0.4000
0.2945	0.0000	-7.0000	0.0000	0.0000	0.0000	0.0000	-0.4000
0.2995	0.0000	-6.0000	0.0000	0.0000	0.0000	0.0000	-0.2780
0.2714	0.0000	-5.0000	0.0000	0.0000	0.0000	0.0000	1.7260
0.2413	0.0000	-4.0000	0.0000	0.0000	0.0000	0.0000	1.7260
0.2069	0.0000	-3.0000	0.0000	0.0000	0.0000	0.0000	1.9820
0.1414	0.0000	-2.0000	0.0000	0.0000	0.0000	0.0000	3.8550
0.0741	0.0000	-1.0000	0.0000	0.0000	0.0000	0.0000	3.8550
0.0001	0.0000	0.0000	0.0000	0.0000	0.0000	0.0000	4.2500
-0.1030	0.0000	1.0000	0.0000	0.0000	0.0000	0.0000	5.9850
-0.2078	0.0000	2.0000	0.0000	0.0000	0.0000	0.0000	5.9850
-0.3217	0.0000	3.0000	0.0000	0.0000	0.0000	0.0000	6.5300
-0.4628	0.0000	4.0000	0.0000	0.0000	0.0000	0.0000	8.1200
-0.6054	0.0000	5.0000	0.0000	0.0000	0.0000	0.0000	8.1200
-0.7600	0.0000	6.0000	0.0000	0.0000	0.0000	0.0000	8.8290
-0.9395	0.0000	7.0000	0.0000	0.0000	0.0000	0.0000	10.2560
-1.1205	0.0000	8.0000	0.0000	0.0000	0.0000	0.0000	10.2560
-1.3167	0.0000	9.0000	0.0000	0.0000	0.0000	0.0000	11.1520
-1.5349	0.0000	10.0000	0.0000	0.0000	0.0000	0.0000	12.3840
-1.7545	0.0000	11.0000	0.0000	0.0000	0.0000	0.0000	12.3840
-1.9936	0.0000	12.0000	0.0000	0.0000	0.0000	0.0000	13.5120
-2.2515	0.0000	13.0000	0.0000	0.0000	0.0000	0.0000	14.5180
-2.5104	0.0000	14.0000	0.0000	0.0000	0.0000	0.0000	14.5180
-2.8107	0.0000	15.0000	0.0000	0.0000	0.0000	0.0000	15.9250
-3.0928	0.0000	16.0000	0.0000	0.0000	0.0000	0.0000	16.6660
-3.3922	0.0000	17.0000	0.0000	0.0000	0.0000	0.0000	16.6660
-3.7229	0.0000	18.0000	0.0000	0.0000	0.0000	0.0000	18.3970
-4.0577	0.0000	19.0000	0.0000	0.0000	0.0000	0.0000	18.8110
-4.4075	0.0000	20.0000	0.0000	0.0000	0.0000	0.0000	18.8110

Appendix VII. C.A.D Drawings

List of ISIS C.A.D drawings used to ascertain the instrument parameters required by VITESS

N.B. The hardcopy of this report contains the actual drawings

Drawings can be obtained from: <http://shad.sci.rl.ac.uk/>

IRIS beam geometry: A1-SI-2525-080-02-G

OSIRIS flight tube assembly: AO-SI-2525-700-01-F

6m disc chopper: A1-SI-2700-395-00-A

140° chopper disc: A1-SI-2700-152-00-A

OSIRIS tile support plate: AO-SI-2526-364-05-E

OSIRIS tile support plate: A0-SI-2526-364-03-F

IRIS tile support plate: A0-SI-2526-522-03-C

This document was created with Win2PDF available at <http://www.daneprairie.com>.
The unregistered version of Win2PDF is for evaluation or non-commercial use only.